

## Stiff Polymers, Foams, and Fiber Networks

Claus Heussinger and Erwin Frey

*Arnold Sommerfeld Center for Theoretical Physics and CeNS, Department of Physics, Ludwig-Maximilians-Universität München, Theresienstrasse 37, D-80333 München, Germany*

*Hahn-Meitner-Institut, Glienicker Strasse 100, D-14109 Berlin, Germany*

(Received 15 March 2005; published 9 January 2006)

We study the elasticity of fibrous materials composed of generalized stiff polymers. It is shown that, in contrast to cellular foamlike structures, affine strain fields are generically unstable. Instead, a subtle interplay between the architecture of the network and the elastic properties of its building blocks leads to intriguing mechanical properties with intermediate asymptotic scaling regimes. We present exhaustive numerical studies based on a finite element method complemented by scaling arguments.

DOI: [10.1103/PhysRevLett.96.017802](https://doi.org/10.1103/PhysRevLett.96.017802)

PACS numbers: 61.41.+e

Cellular and fibrous materials (see Fig. 1) are ubiquitous in nature and in many areas of technology. Examples range from solid or liquid foams over wood and bone to the protein fiber network of cells [1–3]. On a mesoscopic level, these materials are comprised of struts and membranes with anisotropic elastic properties. The systems differ widely in architecture. One finds patterns which are as regular as a honeycomb, as sophisticated as the particular design of a dragonfly’s wing, or simply random [4]. The manifold combinations of architecture and elastic properties of the building blocks allow for a rich spectrum of macroscopic elastic responses. For regular cellular structures, macroscopic elasticity can already be understood by considering the response of a single cell [2,5]. In these systems, local stresses acting on an individual cell are the same as those applied on the macroscopic scale. In other words, the local deformation  $\delta$  of a cell with linear dimension  $l_s$  follows the macroscopic strain  $\gamma$  in an *affine way* such that it scales as  $\delta \propto \gamma l_s$ . Since in affine models there can be no cooperativity between the elastic responses of individual cells, the effect of the assembled structure can be predicted simply by counting the number of cells. Fibrous networks, on the other hand, are dramatically different already in their morphology as can be inferred from Fig. 1. The presence of fibers introduces the additional mesoscopic scale of the fiber length  $l$  and, by hierarchically cutting cells into smaller and smaller compartments, generates a broad distribution of pore sizes that, in contrast to foams, has a nonvanishing weight even for the smallest cells [6]. This difference in architecture crucially affects the mechanical properties. Recently, a nonaffine regime has been identified [7] and characterized [8–10] in two-dimensional networks of classical beams (“Mikado model”) commonly used to model the mechanical properties of paper sheets [11–14]. The nonaffinity of the deformation field necessarily implies that in these networks cooperativity effects play an important role.

In this Letter, we will contrast the two systems of foams and fiber networks and relate their different linear elastic properties to their specific structural features. By system-

atically tuning the force response properties of the individual elements, we will be able to show that the hierarchical architecture of the fiber network leads to a new length scale, below which correlations drive the system away from the state of affine deformations. We will, moreover, describe the mechanism that generates this length and calculate the resulting power law behavior of the elastic modulus by a scaling argument.

The fiber network is defined as follows.  $N$  anisotropic elastic elements, geometrically represented by straight lines of length  $l$ , are placed on a plane of area  $A = L^2$  such that both the position and the orientation of the elements are uniformly randomly distributed. The length of the segments, i.e., the distance  $l_s$  between any two neighboring intersections, follows an exponential distribution [6]

$$P(l_s) = \langle l_s \rangle^{-1} e^{-l_s/\langle l_s \rangle}, \quad (1)$$

with a mean value that is given in terms of the density  $\rho = Nl/A$  as  $\langle l_s \rangle = \pi/2\rho$ . At any intersection, a permanent cross-link with zero extensibility is generated. This constrains the relative translational motion of the two filaments, while leaving the rotational degrees of freedom independent. Not allowing for kinking, filaments are assumed to remain straight at the cross-links. The simplicity of this network structure (one parameter  $\rho$ ) makes it an

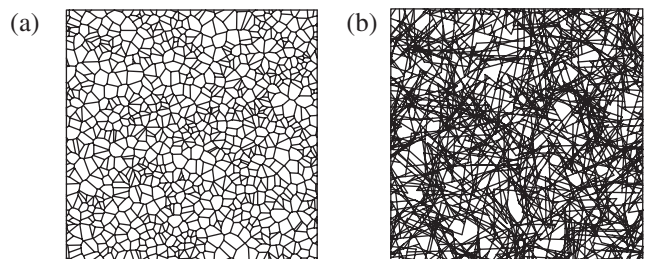


FIG. 1. Illustration of the different architecture of (a) cellular and (b) fibrous materials. The foam in (a) is constructed by a Voronoi tessellation from the centers of the fibers in (b).

ideal candidate to obtain physical insight into the relation of architecture and elastic properties of the constituents, which we specify next. Previous studies [8,9] have considered classical beams of radius  $r$  and bending stiffness  $\kappa$ . Loaded along their axis (“stretching”), such slender rods have a rather high stiffness  $k_s = 4\kappa/l_s r^2$ , while they are much softer with respect to transverse deformations  $k_\perp(l_s) = 3\kappa/l_s^3$  (“bending”). Here we consider elastic elements where, in addition to the mechanical stiffness of beams, a more general stretching coefficient

$$k_\parallel(l_s) = 6\kappa \frac{l_p^\alpha}{l_s^{3+\alpha}} \quad (2)$$

is introduced. This may result from thermal fluctuations of the filament immersed in a heat bath of solvent molecules. The prefactor is chosen such that  $k_\parallel$  for  $\alpha = 1$  reduces to the longitudinal entropic elasticity of a stiff polymer described by the wormlike chain model grafted at one end [15]. In this case, the material length  $l_p$  is called the persistence length of the polymer and quantifies the ratio of bending to thermal energy  $l_p = \kappa/k_B T$ . The phenomenological exponent  $\alpha$  allows us to extend our discussion to the broad class of systems for which  $k_\parallel$  is a monomial (with units energy per area) involving one additional material length  $l_p$ . Having two longitudinal deformation modes, the effective stretching stiffness is equivalent to a serial connection of the “springs”  $k_s$  and  $k_\parallel$ . Setting  $l_p = cr$ , we can write  $k_s \propto k_\parallel (\alpha = -2)$ . The constant  $c$  is a material property of the specific polymer and has been chosen as  $c = 1.5 \times 10^4$ , which roughly corresponds to the biopolymer F-actin. The precise value, however, is irrelevant with regard to the thermal response  $k_\parallel$  and specifies only the location of the crossover to  $k_s$ . The description of a thermally fluctuating network in terms of force constants  $k_\parallel$ ,  $k_s$ , and  $k_\perp$  is in the spirit of a Born-Oppenheimer approximation that neglects the fluctuations of the “slow variables,” the cross-link positions, while assuming the “fast” polymer degrees of freedom to be equilibrated. By minimization of the internal energy with respect to the slow parameters, we calculate the shear modulus  $G$  for a given macroscopic shear strain of  $\gamma = 0.01$ . This procedure is performed with the commercially available finite element solver MSC.MARC using periodic boundary conditions on all four sides of the simulation box.

As indicated in the introduction, the complement to the fiber network is a regular foamlike material that one can describe by a mean-field approach [2,5]. Assuming correlations between neighboring segments to be absent, the response is fully described by the properties of an average segment of length  $\langle l_s \rangle \propto \rho^{-1}$ . Marking the force constants of this segment by an overbar, we can express them in the form (neglecting numerical prefactors)  $\bar{k}_\perp \approx \kappa \rho^3$ ,  $\bar{k}_\parallel \approx \bar{k}_\perp (\rho l_p)^\alpha$ , and  $\bar{k}_s \approx \bar{k}_\perp (\rho r)^{-2}$ , respectively. The deformation modes will act as springs connected in series [5] such that the modulus takes the form

$$G_{\text{foam}}^{-1} = a\bar{k}_\parallel^{-1} + b\bar{k}_\perp^{-1} + c\bar{k}_s^{-1}. \quad (3)$$

The foam will thus show a crossover from thermal stretching to bending at  $l_p \approx \langle l_s \rangle$  and to mechanical stretching at  $r \approx \langle l_s \rangle$ . This behavior, and for illustration also that of a completely random foam, are indicated by the dashed lines in Figs. 2 and 3, where they can be compared with the actual results of our numerical analysis on the fiber system. In Fig. 2, the normalized shear modulus  $G l^3 / \kappa$  is shown as a function of dimensionless persistence length  $l_p / l$  for a set of dimensionless densities  $\rho l$  for the special case of  $\alpha = 1$ . At large  $l_p / l$  (right part of the plot), we recover purely mechanical behavior characterized by  $G \propto \bar{k}_s$  consistent with the mean-field picture of Eq. (3) [8,9,11]. Our main interest, however, lies in the regime of small  $l_p / l$  (left part of the plot), where the persistence length is small enough for thermal fluctuations to become relevant. To analyze the modulus in the thermal regime ( $k_s \rightarrow \infty$ ), it will be helpful to use dimensional analysis and write the modulus in terms of the two remaining response coefficients  $\bar{k}_\perp$  and  $\bar{k}_\parallel$  of an average segment

$$G(\kappa, l, l_p, \rho) = \bar{k}_\perp g(\rho l, \bar{k}_\parallel / \bar{k}_\perp). \quad (4)$$

The first argument of the scaling function  $g$ , the density  $x = \rho l$ , is of geometrical origin and counts the number of cross-links per filament. The second argument,  $y = \bar{k}_\parallel / \bar{k}_\perp \approx \rho l_p$ , relates to the energy balance between stretching and bending of an average segment and marks a crossover at  $y \approx 1$  or  $l_p \approx \langle l_s \rangle$ . From Fig. 2 and the inset in Fig. 3, one infers that for *low densities*  $g = y f(x)$ , implying for the modulus  $G = \bar{k}_\parallel f(\rho l)$ . This linear dependence on the “preaveraged” stretching compliance  $\bar{k}_\parallel$  hints at a foamlike stretching dominated regime [10] where correlations are absent. As one can also infer from these figures, the domain of validity of this linear regime is

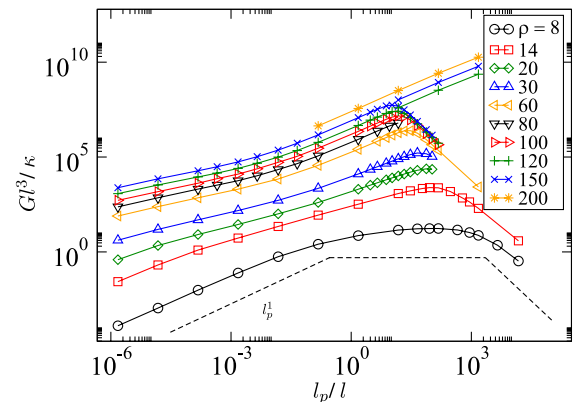


FIG. 2 (color online). Shear modulus  $G l^3 / \kappa$  as function of persistence length  $l_p / l$  for various densities  $\rho l$  and  $\alpha = 1$ . The second branch in the upper right corner ( $\rho l \geq 120$ ) is obtained by suppressing the mechanical response (“ $k_s \rightarrow \infty$ ”). The dashed line indicates the three regimes as obtained by Eq. (3).

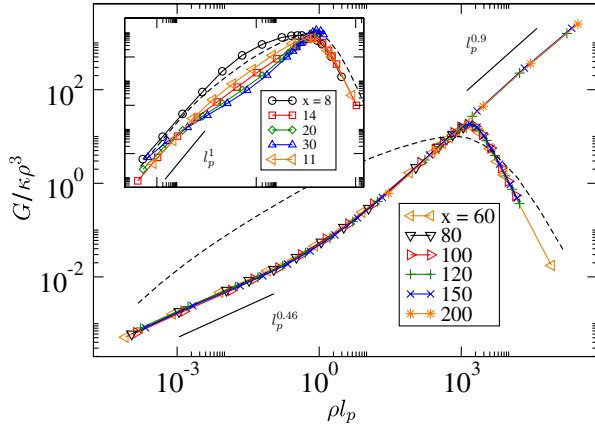


FIG. 3 (color online). Scaling function  $g$  as a function of  $\rho l_p$  for various values of  $x = \rho l$ . For comparison, we present also the scaling function of a *random foam* (dashed line).

extremely narrow and confined to low densities  $x \leq 20$  and persistence lengths  $y \ll 1$ . For *medium and high densities*, Fig. 3 shows two nontrivial scaling regimes where  $g(x \gg 1, y) = y^z$  becomes independent of  $x$  (and, therefore, of the filament length  $l$ ) and exhibits power law behavior with exponents  $z = 0.46$  and  $z = 0.9$  for small and large values of  $y$ , respectively. In both cases, the modulus can be written as a generalized geometric average

$$G \propto \bar{k}_\perp^{1-z} \bar{k}_\parallel^z, \quad (5)$$

which has to be contrasted with Eq. (3), where bending and stretching modes are assumed to superimpose linearly. Here correlation effects between the segments induce the nontrivial form of the modulus and distinguish the fiber network from the ordinary foamlike behavior obtained by single segment considerations. Whereas foams may be considered as a limit where the number of cross-links per fiber is small (filament length identical to the cell size), the scaling limit of fiber networks corresponds to infinite fiber length.

To understand the origin of the correlations, one has to take into account the full distribution of segment lengths, Eq. (1). This will have a pronounced effect on an affine deformation field  $\delta_{\text{aff}} \propto \gamma l_s$ , as can be seen by considering the axial force  $f_\parallel$  along an affinely stretched segment of length  $l_s$ ,  $f_\parallel = k_\parallel \delta_{\text{aff}} \simeq \kappa l_p^\alpha \gamma / l_s^{2+\alpha}$ . In any but the purely mechanical situation, where  $\alpha = -2$  (and, thus,  $f_s \simeq \kappa \gamma / r^2$ ),  $f_\parallel$  strongly depends on the segment length. This implies that, in general, two neighboring segments on the same filament produce a net force at their common node that has to be taken up by the crossing filament which then, preferentially, will start to bend. From the exponential distribution of segment lengths in Eq. (1), one can easily show that the size of these residual forces  $\delta f$  can be arbitrarily large. The corresponding probability distribution  $Q(\delta f)$  shows polynomial (fat) tails

$$Q(\delta f) \propto \delta f^{-(3+\alpha)/(2+\alpha)} P(0), \quad \delta f \rightarrow \infty, \quad (6)$$

and has a diverging mean value. This is due to the finite probability  $P(0) = P(l_s = 0) \neq 0$  of finding segments with zero length. As a consequence, there are always residual forces high enough to cause significant bending of the crossing filament. Hence, we conclude that an affine deformation field is unstable and that the system can easily lower its energy by redistributing the stresses to relieve shorter segments and remove the tails of the residual force distribution  $Q(\delta f)$ .

This mechanism can be used to derive an expression for the modulus in the parameter region  $y \ll 1$ , where the value of the exponent  $z = 0.46$  indicates that bending and stretching deformations contribute equally to the elastic energy. We assume that segments up to a critical length  $l_c$ —to be determined self-consistently—will fully relax from their affine reference state to give all their energy to the neighboring segment on the crossing filament. The energy of segments with  $l_s > l_c$  will then have two contributions: first, a stretching part from the imposed affine strain field (for simplicity, we will set  $\alpha = 1$  in what follows.)

$$w_s(l_s) \simeq k_\parallel \delta_{\text{aff}}^2 \simeq \kappa \gamma^2 \frac{l_p}{l_s}, \quad (7)$$

second, a bending part

$$w_b(l_s) \simeq k_\perp \delta_{\text{aff}}^2 \simeq \kappa \gamma^2 \frac{l_s^2}{l_p^3}, \quad (8)$$

that arises only if the segment under consideration is neighbor to an element on the crossing filament with  $l'_s < l_c$  (the prime refers to the neighboring small segment). Adding both contributions and averaging over all segments  $l_s > l_c$  and  $l'_s < l_c$ , we arrive at the expression  $w \simeq \kappa \gamma^2 \rho (\rho l_p / x_c + x_c)$ , where  $x_c := \rho l_c \ll 1$  in the parameter range of interest. Minimizing with respect to  $x_c$  gives the required expressions  $x_c^{\text{min}} \simeq (l_p \rho)^{1/2}$  and  $G \simeq \rho^2 w_{\text{min}} / \gamma^2 \simeq \kappa \rho^{7/2} l_p^{1/2}$ , corresponding to a value  $z = 1/2$  for the exponent that compares well with the measured value  $z = 0.46$ . Repeating the calculation for general values of  $\alpha$  gives  $z(\alpha) = \alpha / (1 + \alpha)$ . We have verified this result by simulations with an accuracy of about 10% [16]. The nontrivial behavior of  $G$  observed in Figs. 2 and 3 can thus be explained by a length scale  $l_c = \langle l_s \rangle (l_p / \langle l_s \rangle)^{1/2}$ , below which the affinity of the deformation field breaks down. The mechanism is illustrated in Fig. 4, where a histogram for the fraction of energy stored in segments of various lengths is shown. Increasing the persistence length, the short segments one after the other lose their energies in favor of additional excitations in longer segments.

When, eventually,  $l_c \approx l_p \approx \langle l_s \rangle$  ( $y \approx 1$ ), the affine strain field does not serve as a reference configuration any more, since it is strongly perturbed by a majority of

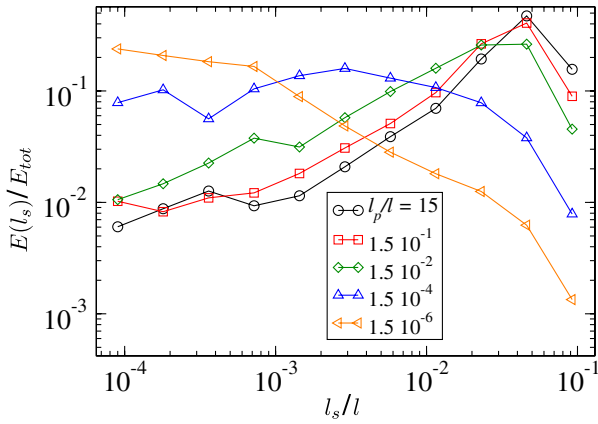


FIG. 4 (color online). Fraction of energy stored in the various segment lengths; the curves correspond to different persistence lengths at a density of  $\rho l = 80$ , equivalent to  $\langle l_s \rangle / l \approx 2 \times 10^{-2}$ .

segments with  $l_s < l_c$ . Moreover, the unloading of the smaller segments now produces significant stretching deformations of their neighbors on the *same* filament such that the available energy for bending of the *crossing* filament is reduced. At this stage, one enters the second intermediate asymptotic regime where, as in the affine regime at low densities, stretching modes dominate the modulus. As can be seen in Fig. 4, only the longest segments carry substantial amounts of energy such that the displacement field must be highly nonaffine. For  $l_p/l \geq 1.5 \times 10^{-2}$ , about 90% of the energy is stored in the longest 30% of the segments. In this parameter range, bending is on average the softer mode  $y = \bar{k}_{\parallel} / \bar{k}_{\perp} \gg 1$  and, therefore, contributes only very little to the total energy. Raising the density to still higher values, it is conceivable from our data that the exponent  $z = 0.9$  approaches  $z = 1$ , which would mean that the energy in the bending modes is completely negligible and  $G \sim \bar{k}_{\parallel}$  as in the affine regime. A transition into a regime dominated by the low-energy bending modes would not be favorable, however. As is known from the mechanical fiber model [8], such a regime must not be characterized by the preaveraged force constant  $\bar{k}_{\perp} = k_{\perp}(\langle l_s \rangle)$  but by an effective stiffness  $\langle k_{\perp} \rangle \approx \kappa / \xi^3$  with a new length scale  $\xi = l(\rho l)^{-\mu/3}$  and  $\mu \approx 6.7$  that is highly dependent on fiber length  $l$ .

In summary, we found that, for a broad range of parameters, the macroscopic shear modulus of fibrous networks is asymptotically independent of the fiber length. Affine stretching is energetically unstable towards a redistribution of energies in favor of longer segments. This gives rise to a correlation-induced elasticity that cannot be explained within a “single cell” model. This physical picture is of general validity and will apply whenever the distribution of segment lengths is sufficiently broad. Cellular systems, being the appropriate structures for rather flexible poly-

mers, will therefore show nonaffine behavior only if they are highly irregular [16–18]. In the complementary case of the fiber network with its hierarchical, scale-invariant architecture, the nonaffinity even leads to asymptotic scaling regimes. These networks are particularly well suited to describe the macroscopic linear response of stiff polymer networks. Therefore, our results may be directly relevant for two-dimensional networks of the filamentous biopolymer F-actin, assembled on top of microfabricated pillars [19]. In addition, it might shed new light on very recent rheological measurements on cross-linked actin networks [20,21], which emphasize the single-polymer origin of the measured elastic moduli. Our simulations, on the contrary, highlight the potentially nontrivial effects of interpolymer correlations on the macroscopic elasticity.

- [1] D. Weaire and S. Hutzler, *The Physics of Foams* (Oxford University Press, Oxford, 2001).
- [2] L. J. Gibson and M. F. Ashby, *Cellular Solids: Structure and Properties* (Cambridge University Press, Cambridge, England, 1999).
- [3] B. Alberts *et al.*, *Molecular Biology of the Cell* (Garland Publishing, New York, 1994).
- [4] D. W. Thompson, *On Growth and Form* (Cambridge University Press, Cambridge, England, 1961).
- [5] A. M. Kraynik and W. E. Warren, in *Low Density Cellular Plastics*, edited by H. Hilyard and C. Cunningham (Kluwer Academic, Amsterdam, 1994), Chap. 7.
- [6] O. Kallmes and H. Corte, *Tappi* **43**, 737 (1960).
- [7] E. Frey, K. Kroy, J. Wilhelm, and E. Sackmann, in *Dynamical Networks in Physics and Biology*, edited by G. Forgacs and D. Beysens (Springer, Berlin, 1998).
- [8] J. Wilhelm and E. Frey, *Phys. Rev. Lett.* **91**, 108103 (2003).
- [9] D. A. Head, A. J. Levine, and F. C. MacKintosh, *Phys. Rev. Lett.* **91**, 108102 (2003).
- [10] D. A. Head, A. J. Levine, and F. C. MacKintosh, *Phys. Rev. E* **68**, 061907 (2003).
- [11] J. A. Åström, J. P. Mäkinen, M. J. Alava, and J. Timonen, *Phys. Rev. E* **61**, 5550 (2000).
- [12] J. A. Åström, S. Saarinen, K. Niskanen, and J. Kurkijärvi, *J. Appl. Phys.* **75**, 2383 (1994).
- [13] M. Latva-Kokko and J. Timonen, *Phys. Rev. E* **64**, 066117 (2001).
- [14] S. Heyden, Ph.D. thesis, Lund University, 1996.
- [15] K. Kroy and E. Frey, *Phys. Rev. Lett.* **77**, 306 (1996).
- [16] C. Heussinger and E. Frey, cond-mat/0512557.
- [17] A. Fazekas, R. Dendievel, L. Salvo, and Y. Bréchet, *Int. J. Mech. Sci.* **44**, 2047 (2002).
- [18] M. J. Silva, W. C. Hayes, and L. J. Gibson, *Int. J. Mech. Sci.* **37**, 1161 (1995).
- [19] W. H. Roos *et al.*, *Chem. Phys. Chem.* **4**, 872 (2003).
- [20] M. L. Gardel *et al.*, *Science* **304**, 1301 (2004).
- [21] J. H. Shin *et al.*, *Proc. Natl. Acad. Sci. U.S.A.* **101**, 9636 (2004).